REDUCTION OF ETHANOL EMISSIONS USING MANGANESE OXIDES SUPPORTED METALLIC MONOLITHS: A PILOT-SCALE PLANT STUDY.

M.A. PELUSO†, J.E. SAMBETH†, and H. THOMAS‡

† *Centro de Investigación y Desarrollo en Ciencias Aplicadas (CINDECA), La Plata, 1900, Argentina.*
apelu@quimica.unlp.edu.ar
‡ *PlaPiMu (CICPBA-UNLP), M.B. Gonnet, Argentina.*

***Abstract*— Metallic monoliths were prepared by anodized aluminum-scale pilot plant, using sulfuric acid as electrolyte. Anodisation tests were conducted at different times and different temperatures of the electrolytic bath. Aluminum monolith anodized at 40ºC for 30 min was selected for catalysts support. The monoliths were impregnated by two methods: i) impregnation in two stages using two Mn salts in an aqueous medium, and ii) impregnation using a $KMnO_4$ solution in acetone. The last monolith presented a higher and a more homogeneous deposit of manganese oxide layer. The catalytic activity was tested in the total oxidation reaction of ethanol in a pilot-scale reactor at 50 L min^{-1}, and ethanol concentrations of 900, 1800 and 3600 ppm. Monolith impregnated using acetone solution was more active that prepared in aqueous solution in all the experiments carried out.**

***Keywords*— MnO_x; Pilot-scale plant; metallic monoliths; VOCs.**

I. INTRODUCTION

Volatile organic compound (VOCs) emissions, produced from industrial processes, mobile sources, etc., are considered to be severe air pollutants. Catalytic oxidation is one of the most attractive routes for the elimination of VOC emissions. Noble metals (Pt, Pd) or transition metal based-oxides (Mn, Cu, Co, Fe, Ni) are commonly used as active phases (Alifanti *et al*., 2005; Luo *et al*., 2007; Peluso *et al.,* 2008a). Metal oxides have lower activity than noble metal catalysts but they are cheaper and have greater resistance to some poisons (Avila *et al.,* 2005). Among the transition metal oxides of interest for VOC oxidation, MnO_x-based materials exhibited great potential (Craciun *et al.,* 2003).

For environmental applications, high flow rates should be treated and a low-pressure drop is required. For that reason, the catalytic system most widely used for catalytic VOC oxidation is the monolithic reactor.

Metallic monoliths present higher mechanical resistance and thermal conductivity, thinner walls and lower pressure drop than those in ceramics. Additionally, metallic substrates are produced easily and in different and complicated forms adapted to a wide variety of uses (Twing and Webster, 1998).

Aluminum monoliths are generally produced by anodic oxidation, in which a porous alumina layer is obtained on the aluminum surface. The alumina texture can be controlled modifying anodisation parameters such as the current density and the temperature (Burgos *et al.,* 2002). These authors deposited Pt over 6 cm^3 volume Al_2O_3/Al monoliths to study the combustion of VOCs. Barrio *et al*. (2005) studied the impregnation of Al_2O_3/Al monoliths at lab scale with $KMnO_4$ using acetone and water as solvent. They found that pore sealing of alumina occurs in water solutions. However, this is prevented by the use of acetone.

A pilot-scale plant is used to test catalyst at operating conditions similar to the ones existing in to real gas turbine burners. Some works at pilot-scale plant are found using ceramic monoliths (Alvarez *et al*., 2002; Requies *et al*., 2008) but no metallic ones.

The aim of this work is to study the anodisation parameters to obtain metallic monoliths at higher dimensions than are usually found in lab scales, in order to prepare active catalysts for VOC oxidation with non-noble additives such as MnO_x. The prepared monoliths were tested in a pilot-scale plant using catalytic oxidation of ethanol as test reaction.

II. METHODS

A. Sample Preparation

Cylindrical monolith supports were prepared by anodisation of 120 cm x 5 cm aluminum foils of 100 μm thick. Each foil was first washed with water and degreased with acetone. Anodisation was carried out in a longitudinal glass tank with 2.55M sulphuric acid, which is placed in second glass tank contained water. All the experiments were carried out with a current density of 4 A dm^{-2} and during 30 min. The electrolyte temperature used was 20, 30 and 40 ºC. The aluminum sheet was fixed to the anode (working anode) between two aluminum foils connected to the cathode (counterelectrodes). The distance between electrodes was 5 cm. Agitation was provided by a pump which recirculates the electrolyte inside the bath. Temperature control of +/- 0.5ºC was obtained with a refrigerating system and an electrical heater with an On-Off temperature controller. After anodising, aluminum foils were removed from the electrolytic bath, thoroughly washed with water to remove the acid, and then dried at 100 ºC for 1h. Flat and corrugated foils were anodized separately and then both sheets were rolled together to form monoliths. Once the monoliths were prepared, they

were calcined at 500 ºC for 2h. Final monoliths were cylindrical of 5 cm high, and 4.5 cm in diameter and a geometrical volume of 79.5 cm^3, and a cell density of 90 cpsi.

Two different catalytic monoliths were prepared. The first one was prepared by a two-step impregnation method, according to Peluso *et al*. (2008a). Monolith was wet impregnated in a $KMnO_4$ solution, stirred for 60 min and dried. Then it was impregnated with a $Mn(NO_3)_2$ solution, stirred for 60 min and dried again. Finally, it was calcined at 500ºC for 2 h. This monolith was called $MnO_x(aq)$/Al (MnO_x deposited on Al monolith from aqueous solution). In the other preparation the monolith was introduced in acetone and solid $KMnO_4$ was added in order to obtain a 0.66 M solution. The solution with the monolith was stirred for 60 min. Then, the monolith was dried, and finally calcined in air at 500 ºC for 2 h. This monolith was called $MnO_x(org)$/Al (MnO_x deposited on Al monolith from organic solution).

B. Characterization

The amount of alumina generated during anodisation was determined by gravimetry (accuracy better than 3%). It was calculated from the weight difference between the anodised aluminium sheets before and after chemical treatment that selectively dissolved the alumina. The dissolving solution contained 35ml of phosphoric acid and 20g of chromic acid dissolved in distilled water to 1 liter. The dissolution process was carried out at 80 ºC for 10 minutes (Lizarbe Ruiz, 1984).

Taking into account the monoliths dimensions, the characterization of the prepared manganese loading monoliths were carried out using small pieces of crushed monoliths.

Textural properties of the monoliths were measured by N_2 adsorption at the liquid nitrogen temperature (77 K) in a Micromeritics Accussorb 2100 D sorptometer using Surface micrographs of the monoliths and elemental composition and distribution were measured by EDS-SEM using a Phillips SEM 505 microscope. Phase composition was studied by XRD using a Phillips PW 1390 diffractometer with Ni-filtered Cu Kα radiation. X-ray photoelectron spectra (XPS) of the compounds were obtained using a multi-technique system (SPECS) equipped with a dual Mg/Al X-ray source and a hemispherical PHOIBOS 150 analyzer operating in the fixed analyzer transmission (FAT) mode. Binding energies (BE: +-0.1 eV) were calculated using the adventitious hydrocarbon (C (1s) = 284.6 eV) as the internal reference.

C. Catalytic activity

A pilot scale plant was used in order to test the catalysts at operating conditions similar to those existing in real burners. Ethanol was chosen to represent VOC, as it is a typical contaminant of fermentation, liquors and wine industries. Catalytic test was carried out at atmospheric pressure in a continuous tubular stainless steel reactor (Fig. 1) of 150 cm high and 4.5 cm in inner diameter and placed inside a heating furnace that is controlled by 5 independent electrical heaters.

Table 1: Textural properties of prepared alumina.

Temp. (ºC)	gAl_2O_3 mAl^{-2}	Smonolith (m^2 mAl^{-2})	S_{BET} (m^2 g $Al_2O_3^{-1}$)	Vp (cm^3 mAl^{-2})	Dp (Å)
20	13	590	46	2.8	154
30	29	650	23	3.1	160
40	43	938	22	5.0	164

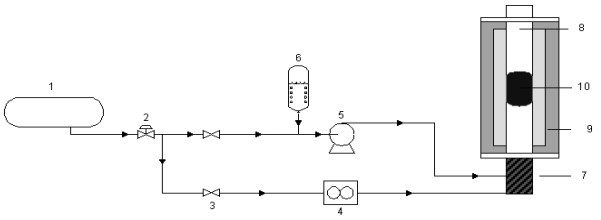

Fig.1- Experimental set-up used for the catalytic ethanol oxidation experiments. (1) Air from compressor; (2) control valves; (3) switch valves; (4) mass flow controller; (5) pump; (6) ethanol reservoir; (7) pre-heater; (8) reactor; (9) furnace; (10) monolith.

Two monoliths were placed on an inert alumina packed bed of 50 cm in height which is used to preheat the gas stream. Temperature was measured using K type thermocouples in the center of the inlet face of the monoliths and in five zones of the furnace inner wall (set point for temperature control). Air from a compressor was mixed with the VOC stream that was evaporated by heating. Total gas flow of ethanol-air was 50000 cm^3 min^{-1} (GSVH 19000 h^{-1}) and the working temperatures were between 100 and 500 ºC. The feed composition was 900, 1800 and 3600 ppm of ethanol in air, with an excess of O_2. Under such conditions, reactor without monolith showed no activity. Conversion was calculated by measuring ethanol disappearance by Gas Chromatography (Shimadzu GC9A), together with the CO_2 measurement by an on-line IR detector (Telaire T6613). Prior to reaction tests, catalysts were pre-treated in air at 500 ºC for 1 hour.

III. RESULTS AND DISCUSSION

A. Monoliths Characterization

The influence of anodisation temperature on the amount of alumina generated by anodisation is shown in Table 1. The amount of alumina electro-generated and the specific surface of the monoliths increased when temperature was increased from 20 to 40 ^oC. However, the specific surface of the alumina decreased when electrolyte temperature was increased. This decrease was attributed to the decrease in the surface pore density, since the pore diameter and the total pore volume increased. Even if the specific surface area of the alumina decreased, this decrease was largely compensated by the increment of the generated alumina, resulting in an increment of the total alumina surface per square meter of aluminum.

Surface morphology of the materials was studied by SEM. Fig. 2(a) shows the surface of the raw material (aluminum sheet) as received from the manufacturer. The surface is smooth and straight. There was a drastic

change in the surface roughness after the anodisation process. At 20 ^{o}C, the surface was completely covered by irregular slits with crests (Fig. 2(b)). As temperature increased from 20 to 40 ^{o}C, (Fig. 2 (c) and (d)) the same surface morphology was observed but at larger scale. This increase is parallel to the increase in the amount of generated alumina. As a consequence, monoliths were prepared with alumina anodized at 40 ^{o}C.

The amount of manganese oxide loaded on the monolith was calculated by weight difference before and after preparation. The deposited amount was 0.65 g for the aqueous preparation and 1.03 g for the preparation with technical grade acetone. Monolith prepared in acetone presented homogeneous black color. Nevertheless, the monolith prepared in water showed a very heterogeneous dark brown to almost white color, presenting points where clearly manganese oxide accumulated (results not shown).

Textural properties of the parent and manganese loaded monoliths are shown in Table 2. After impregnation in water, there was a dramatic change in the textural properties of the monolith. In addition to the decreased specific area, a dramatic diminution of the pore volume and mean pore diameter is noted, indicating a narrowing of the pore mouth (Barrio *et al*., 2005) In the case of the monoliths prepared using acetone there is also a decrease in the textural properties. Nevertheless, the diminution in the pore volume and pore diameter is lower than that of the monoliths impregnated using aqueous solutions.

Surface roughness of the monoliths impregnated with manganese was studied by SEM and elemental composition and distribution were studied by EDS. Results are shown in Table 3 and Fig. 3. Since monolith prepared in water showed a non homogeneous surface deposition, SEM and EDS analysis were performed in two zones of that monolith: brown and almost white zones. The study was also performed in two different zones of MnO_x(*org*)/Al monolith. The brown zone of the MnO_x(*aq*)/Al had an almost twice higher Mn concentration than the white zone, showing the non-homogeneous coating of the manganese layer. On the other hand, monolith MnO_x(*org*)/Al presented a homogeneous surface with higher manganese concentration than the richest manganese zone of the MnO_x(*aq*)/Al monolith. Potassium concentration was also higher in MnO_x(*org*)/Al than in MnO_x(*aq*)/Al. In addition, sulfur was present because of the use of H_2SO_4 during the anodization process.

The higher K concentration of MnO_x(*org*)/Al could be due on the one hand to the higher catalyst mass loaded and to the other hand to the fact that the soluble KNO_3 formed in an aqueous medium was washed.

Mn distribution was uniform all along the sheet, being more populated in MnO_x(*org*)/Al than in MnO_x(*aq*)/Al in agreement with EDS analyses.

Table 2: Textural properties of monoliths.

Monolith	S_{BET} (m^2 mAl^{-2})	Vp (cm^3 mAl^{-2})	Dp (Å)
Al_2O_3/Al	938	5.0	164
MnO_x(*aq*)/Al	760	3.0	127
MnO_x(*org*)/Al	640	3.4	149

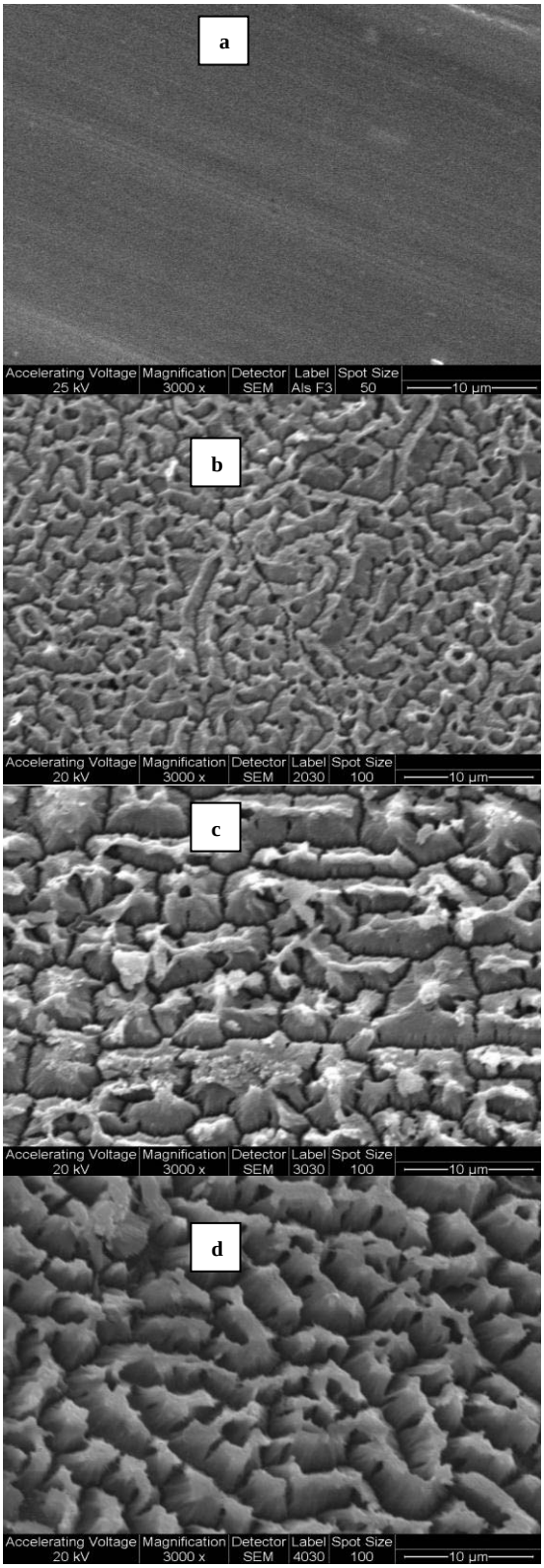

Fig. 2- SEM micrographs of the top view of Al_2O_3/Al prepared: (a) Al; (b) 20 ^{o}C; (c) 30 ºC and (d) 40 ºC.

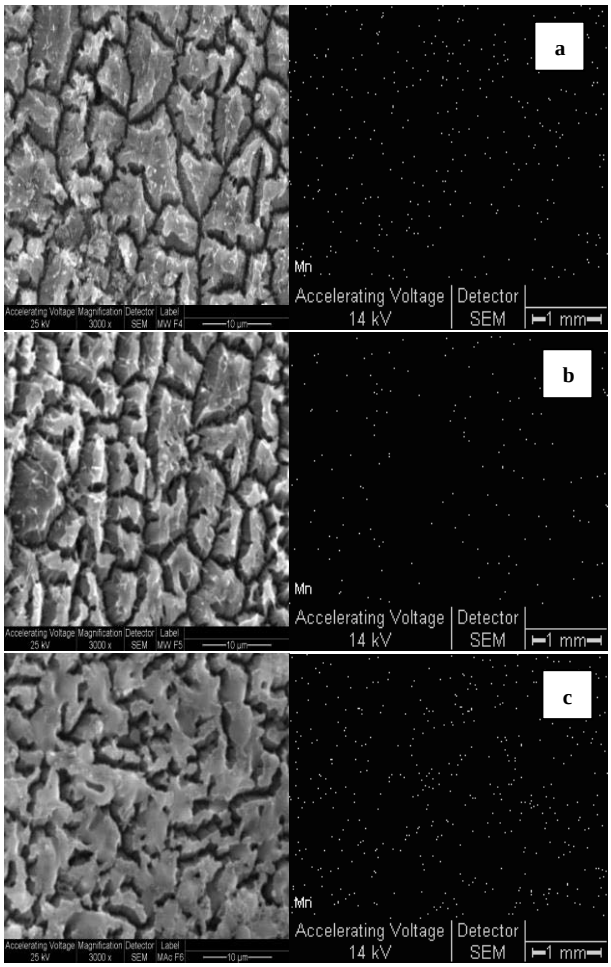

Fig. 3- SEM micrographs of the top view and Mn distribution of $MnO_x/Al_2O_3/Al$ monoliths: (a) $MnO_x(aq)$/Al brown zone; (b) $MnO_x(aq)$/Al white zone and (c) $MnO_x(org)$/Al.

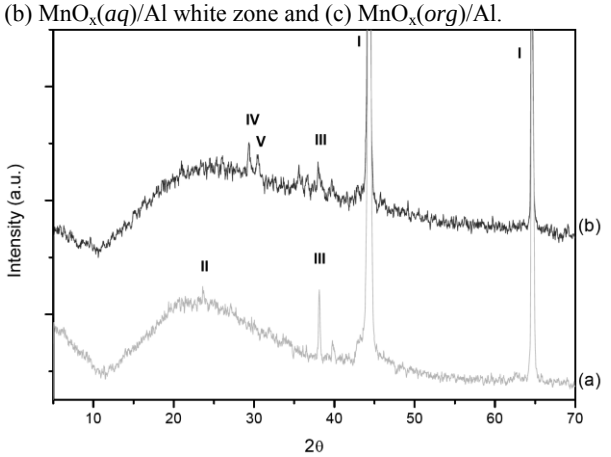

Fig.4- XRD patterns of $MnO_x/Al_2O_3/Al$ monoliths: (a) $MnO_x(aq)$/Al, (b) $MnO_x(org)$/Al. Lines: I = Al (04-0787); II = Mn_2O_3 (78-0390); III = MnO_2 (72-1984); IV = $KMnO_2$ (75-2171); V= K_2SO_4 (83-0682);

Table 3: Chemical composition (wt %) from SEM-EDS analysis

Monolith	O	Al	S	Mn	K
$MnO_x(aq)$/Al *white zone*	59.3	34.7	3.7	2.3	0.1
$MnO_x(aq)$/Al *brown zone*	56.7	34.0	4.3	4.9	0.1
$MnO_x(org)$/Al *zone 1*	55.9	24.5	5.9	5.7	7.9
$MnO_x(org)$/Al *zone 2*	55.8	24.4	6.0	5.8	7.9

Table 4. XPS results of monoliths.

Monolith	$Mn2p_{3/2}$ (eV)	O1s (eV)
$MnO_x(aq)$/Al	641.8 Mn^{3+}(52%)	530.7 O^{2-}(35%)
	643.1 Mn^{4+}(48%)	532.6 OH^-(65%)
$MnO_x(org)$/Al	641.8 Mn^{3+}(30%)	530.2 O^{2-}(81%)
	643.2 Mn^{4+}(54%)	532.0 OH^-(19%)
	645.3 Mn^{7+}(16%)	

X-Ray diffraction patterns of monolith are shown in Fig. 4. Both monoliths show diffraction lines at 2θ = 44.4 and 64.7º corresponding to metallic aluminum. Monolith prepared in aqueous medium shows diffraction lines at 2θ = 24 and 38º characteristic of α-Mn_2O_3 and MnO_2, respectively. On the other hand, $MnO_x(org)$/Al monolith presents a different pattern characterized by diffraction lines at 29 and 30º corresponding to mixed potassium and manganese oxides ($KMnO_2$ and K_3MnO_4) and a line at 38º corresponding to MnO_2.

On the other hand, diffraction lines corresponding to sulfate such as $K_2S_2O_7$, K_2SO_4, appeared in the $MnO_x(org)$/Al monolith. These resulted from the anodisation in H_2SO_4.

As the produced manganese oxide phase was in small amounts and the manganese phases are usually non- stoichiometric, it was difficult to identify it only by means of XRD, therefore XPS studies were performed.

The oxidation state of the Mn species on the monolith surface was analyzed by XPS. Peak intensities were evaluated by applying the peak synthesis procedure (Ponce *et al*., 2000). As a general rule, when a metal or a metal oxide phase is deposited on a support surface, where it develops a strong metal (oxide)–support interaction, the binding energy of core-levels of the supported element (Mn 2p in this work) is shifted a few tenths of eV toward higher binding energies with respect to the bulk oxide (MnO_2 or Mn_2O_3 here) (Cubeiro and Fierro, 1998).

XPS results are summarized in Table 4. In the XPS analyses of the $MnO_x(aq)$/Al monolith, the Mn2*p*, O1*s*, C1*s*, Al2*s* and Al2*p* signals were recorded. The $Mn2p_{3/2}$ is centered at 642.2 eV and deconvoluted in two peaks with BE around 641.8 and 643.1 which are in the range of that reported for Mn_2O_3 (641.3–641.8 eV) and Mn^{4+} ions, respectively (de la Peña O'Shea *et al*., 2004; Obalová *et al.,* 2007). The O1*s* peak was composed by two components. The binding energy of 530.7 eV is characteristic of lattice oxygen (O^{2-}) and the binding energy of 532.6 eV could be assigned to OH^- species (Wang and Li, 2010).

XPS analysis of $MnO_x(org)$/Al monolith detected the presence of Mn2*p*, O1*s*, C1s, K2*p*, Al2*s* and Al2*p* signals. The deconvolution of the $Mn2p_{3/2}$ electron binding energy peak (centered at 643.0 eV) included components centered at 641.8, 643.2 and 645.3 eV attributed to Mn^{3+}, Mn^{4+} and Mn^{7+}, respectively (Obalova *et al.,* 2007; Wollner, 1993). This result is in according to Oku *et al.* (1999) who have reported that the $Mn2p_{3/2}$ binding energy of $KMnO_4$ is in the range of 645–646 eV. The presence of Mn^{7+} can be related to the detection of the K2*p* signal, pointing to an incomplete reaction. The O1s

was split into two components at 530.2 and 532.0 eV, assigned to lattice oxygen and hydroxyl groups, respectively. The presence of Mn^{3+} and Mn^{4+} was also found in the XRD experiments. The presence of Mn^{7+} was only detected in XPS. This could be due to the fact that XRD is a bulk technique and XPS is a more superficial technique, and also manganese oxides are usually non-stoichiometric and present several oxidation states.

B. Catalytic activity

Catalytic tests were performed at a total flow of 50000 cm^3 min^{-1}, corresponding to a specific velocity of 162 cm $seg^{-1}$and a Reynolds number of 402. This value is in agreement with those normally used in catalytic converters (Loayza Perez, 2003).

In all samples tested, CO_2, H_2O and acetaldehyde were formed during ethanol oxidation, and no other partial oxidation products were detected. Acetaldehyde was observed at conversion values below 40%. Preliminary experiments with two Al_2O_3/Al monoliths placed in the reactor did not show any activity for the oxidation of ethanol.

The catalytic activity at different ethanol concentrations are shown in Figs. 5 and 6 for MnO_x(*aq*)/Al and MnO_x(*org*)/Al monoliths, respectively. When increasing ethanol concentration from 900 to 1800 ppm, and from 1800 to 3600 ppm, catalytic activity decreased in both catalysts, being MnO_x(*org*)/Al more active catalysts than MnO_x(*aq*)/Al throughout all tests carried out with the same ethanol concentration. For the MnO_x(*org*)/Al monolith there is a markedly dependence of ethanol concentrations when it is raised from 900 to 1800 ppm, with a difference in the T_{90} of about 40 ºC. From 1800 to 3600 ppm, the ignition curves are somewhat similar, with a difference in the T_{90} of 9 ºC.

In both catalysts there is evidence of the presence of the pair Mn^{4+} - Mn^{3+}, which is claimed to be related to the activity of manganese oxides (Peluso *et al*., 2008b).

On the other hand, potassium is claimed to be a very useful modifying alkali metal, which improves properties of various oxide catalysts (Chen and Zheng, 2004; Zhang *et al*., 2007).

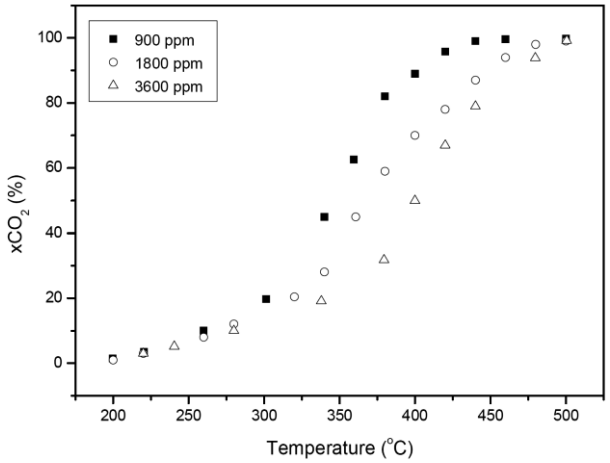

Fig. 5- Ignition curves of ethanol over MnO_x(*aq*)/Al monolith at different ethanol concentrations.

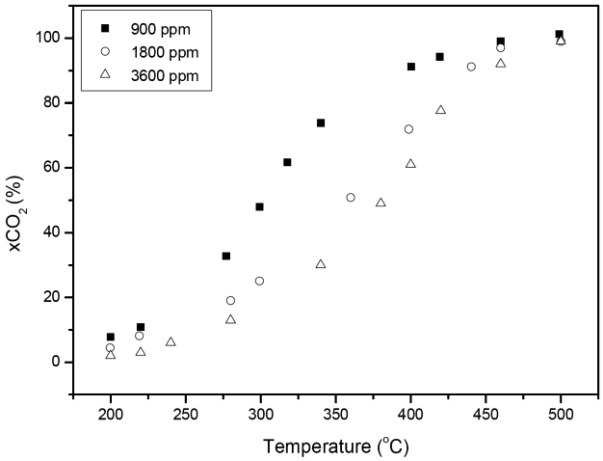

Fig. 6- Ignition curves of ethanol over MnO_x(*org*)/Al monolith at different ethanol concentrations.

Although the manganese oxide formed in both catalyst is not the same, the higher potassium and manganese oxide concentration, in addition to the more homogeneous distribution of the active phase made the MnO_x(*org*)/Al monolith presents a higher ethanol conversion than MnO_x(*aq*)/Al monolith.

MnO_x/Al_2O_3/Al monoliths showed a remarkable stability during laboratory and pilot plant tests .In an isothermal stability test (50000 cm^3 min^{-1} of air containing 3600 ppm of ethanol) carried out at 400 ºC, the conversion remained stable at 60% conversion for 48 hours.

IV. CONCLUSIONS

Al_2O_3/Al monolithic devices for using in a pilot plant were prepared by anodisation of Al sheet. Different tests varying bath temperature were carried out choosing the test performed at 40 ºC for 30 min. MnO_x/Al_2O_3/Al catalysts were prepared by impregnation of supports with aqueous and acetone manganese solutions. Impregnation using acetone as solvent produced a more reproducible, more uniform and higher load of manganese. The catalytic devices synthesized were active in the combustion of ethanol in a pilot-scale plant. The higher the manganese loads on the monolith, the higher the activity. The catalytic activity decrees with the increase in the ethanol concentration. MnO_x/Al_2O_3/Al monoliths are efficient in remove VOCs in pilot scale plant, and are promising catalysts for VOCs elimination in real plants.

REFERENCES

Alifanti, M., M. Florea, S. Somacescu and V. Parvulescu, "Supported perovskites for total oxidation of toluene," *Appl.Catal. B*, **60**, 33-39 (2005).

Alvarez, E., J. Blanco, J. Otero De Becerra, J. Olivares Del Valle and L. Salvador, "Platinum monolithic catalyst for SO_2 abatement in dust-free flue-gas from combustion units," *Lat. Am. Appl. Res.*, **32**, 123-129 (2002).

Avila, P., M. Montes and E. Miro, "Monolithic reactor for environmental applications. A review on preparation technologies," *Chem. Eng. J.*, **109**, 11-36 (2005).

Barrio, I., I. Legorburu, M. Montes, M. Domínguez, M. Centeno and J.A. Odriozola, "New redox deposition-precipitation method for preparation of supported manganese oxide catalysts," *Catal. Letters*, **101**, 151-157 (2005).

Burgos, N., M. Paulis, M. Antxustegui and M. Montes, "Deep oxidation of VOC mixtures with platinum supported on Al_2O_3/Al monoliths," *Appl. Catal. B*, **38**, 251-258 (2002).

Chen, M. and X. Zheng, "The effect of K and Al over $NiCo_2O_4$catalyst on its character and catalytic oxidation of VOCs," *J. Mol. Catal. A,* **221**, 77-80 (2004).

Craciun, R., B. Nentwick, K. Hadjiivanov and H. Knözinger, "Structure and redox properties of MnO*x*/ Yttrium-stabilized zirconia (YSZ) catalyst and its use in CO and CH_4 oxidation," *Appl. Catal. A,* **243**, 67-79 (2003).

Cubeiro, M. and J. Fierro, "Selective Production of Hydrogen by Partial Oxidation of Methanol over ZnO-Supported Palladium Catalysts," *J. Catal.*, **179**, 150-162 (1998).

de la Peña O'Shea, V., M. Alvarez-Galvàn, J. Fierro and P. Arias, "Influence of feed composition on the activity of Mn and $PdMn/Al_2O_3$ catalysts for combustion of formaldehyde/methanol," *Appl. Catal. B*, **57**, 191-199 (2004).

Lizarbe Ruiz, L.; "Oxidación Anódica, Coloración y Sellado del Aluminio," in *Teoría y Práctica de la Lucha Contra la Corrosión*, Ed. J.A. González Fernández, Grafimad S.A., Madrid (1984).

Loayza Perez, L., "Diseño de un incinerador catalítico," *Rev. Per. Quim. Ing. Quim.,* **5**, 3-10 (2003).

Luo, M., M. He, Y. Xie, P. Fang and J. Jin, "Toluene oxidation on Pd catalysts supported by CeO_2–Y_2O_3 washcoated cordierite honeycomb," *Appl. Catal. B*, **69**, 213-218 (2007).

Obalová, K. Pacultová, J. Balabánová, K. Jirátová, Z. Bastl, M. Valášková, Z. Lacný and F. Kovanda, "Effect of Mn/Al ratio in Co–Mn–Al mixed oxide catalysts prepared from hydrotalcite-like precursors on catalytic decomposition of N_2O," *Catal. Today*, **119**, 233-238 (2007).

Oku, M., K. Wagatsuma and T. Konishi, "Relation between 2p X-ray photoelectron and Kα X-ray emission spectra of manganese and iron oxides," *J. of Electron Spectroscopy and Related Phenomena*, **98–99**, 277-285 (1999).

Peluso, M., E. Pronsato, J. Sambeth, G. Busca and H. Thomas, "Catalytic combustion of ethanol on pure and alumina supported K-Mn oxides: An IR and flow reactor study," *Appl. Catal. B*, **78**, 73-79 (2008a).

Peluso, M.A., L. Gambaro, E. Pronsato, D. Gazzoli H. Thomas and J. Sambeth, "Synthesis and catalytic activity of manganese dioxide (type OMS-2) for the abatement of oxygenated VOCs," *Catal. Today*, **133**, 487-492 (2008b).

Ponce, S., M. Peña and J. Fierro, "Surface properties and catalytic performance in methane combustion of Sr-substituted lanthanum manganites," *Appl. Catal. B*, **24**, 193-205 (2000).

Requies, J., M. Alvarez-Galvan, V. Barrio, P. Arias, J. Cambra, M. Güemes, M. Carrera, V. de la Peña O`Shea and J. Fierro, "Palladium-manganese catalysts supported on monolith systems for methane combustion," *Appl. Catal. B,* **79**, 122-131 (2008).

Twing, M. and D. Webster, *Structure Catalysts and Reactors,* Marcel Dekker: New York (1998).

Wang, R. and J. Li, "Effects of precursor and sulfation on OMS-2 catalysts for oxidation of ethanol and acetaldehyde at low temperature," *Environ. Sci. Technol.,* **44**, 4282–4287 (2010).

Wollner, A., F. Lange, J. Schemlz and H. Knozinger, "Characterization of mixed copper-manganese oxides supported on titania catalysts for selective oxidation of ammonia," *Appl. Catal. A,* **94**, 181-203 (1993).

Zhang, Z., Z. Mou, P.Yu, Y. Zhang and X. Ni, "Diesel soot combustion on potassium promoted hydrotalcite-based mixed oxide catalysts," *Catal. Commun.*, **8**, 1621-1624 (2007).

Received: August 24, 2012
Accepted: March 26, 2013
Recommended by Subject Editor: Pedro de Alcântara Pessôa